Volume 10 | Number 19 | 21 May 2018 | Pages 8875–9412

Nanoscale

rsc.li/nanoscale

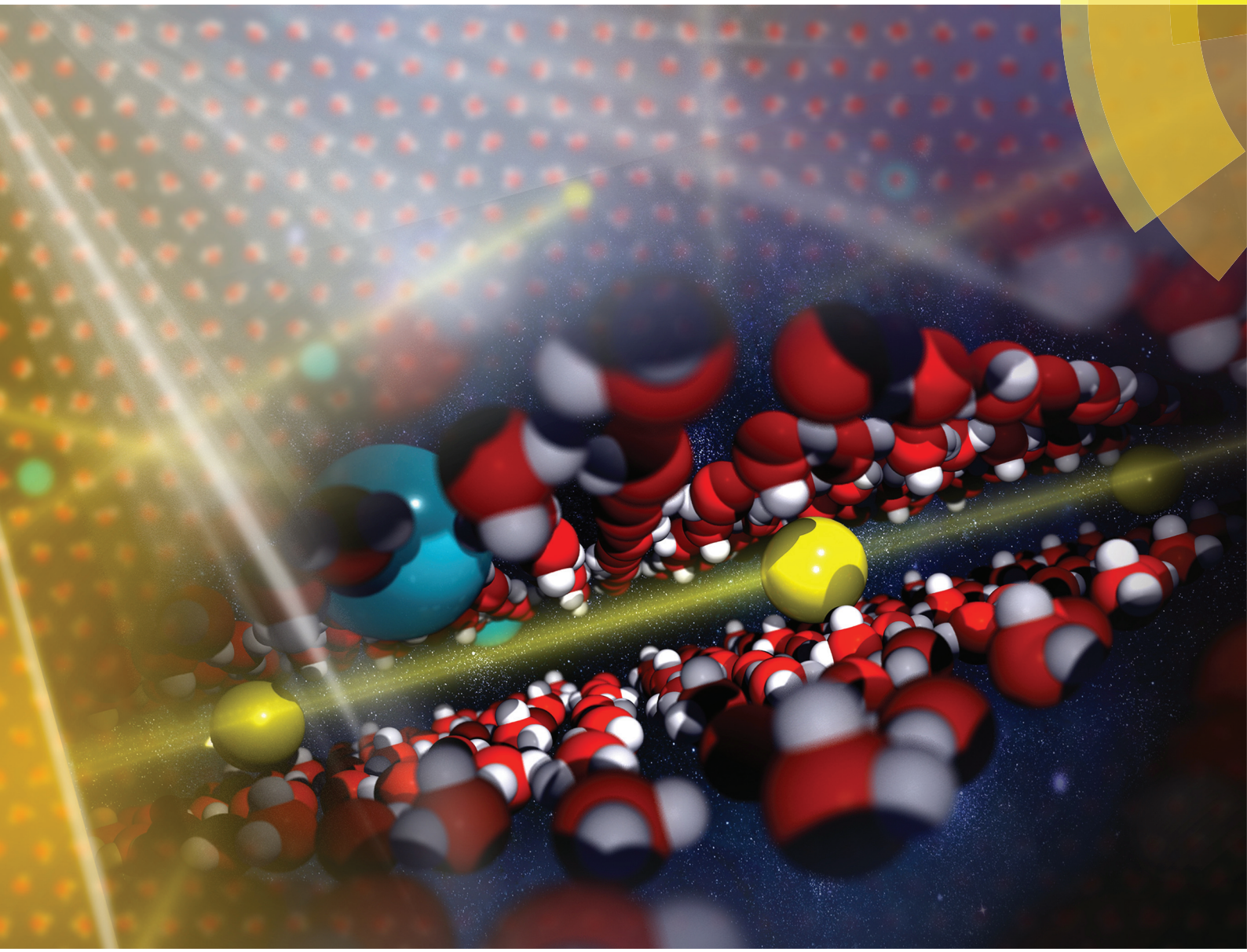

ISSN 2040-3372

ROYAL SOCIETY OF CHEMISTRY

PAPER
Hu Qiu, Wanlin Guo *et al.*
Anomalous cation diffusion in salt-doped confined bilayer ice

NCNST

Nanoscale

PAPER

View Article Online
View Journal | View Issue

Cite this: *Nanoscale*, 2018, **10**, 8962

Anomalous cation diffusion in salt-doped confined bilayer ice†

Hu Qiu, * Minmin Xue, Chun Shen and Wanlin Guo*

Received 13th February 2018,
Accepted 28th March 2018

DOI: 10.1039/c8nr01301b

rsc.li/nanoscale

The diffusive dynamics of aqueous electrolyte solutions in nanoconfined spaces has attracted considerable attention due to their potential applications in desalination, biosensors and supercapacitors. Here we show by molecular dynamics simulations that lithium and sodium ions diffuse at a rate at least an order of magnitude higher than that of water molecules when the ions are trapped in an ice bilayer confined between two parallel plates. This novel picture is in sharp contrast to the prevailing view that the diffusion rate of ions is comparable to or even lower than that of water in both bulk and confined solutions. The predicted high ion mobility stems from frequent lateral hopping of ions along the coordination sites inside the hydrogen-bonding network connecting the two water layers of the ice bilayer. This anomalous diffusion should provide new insights into the physics of confined aqueous electrolytes.

1. Introduction

Knowing the properties of aqueous electrolytes in nanoscale spaces is key to understanding important biological processes such as ion transport across biological channel proteins as well as to developing useful technologies for their applications in desalination,[1,2] biosensors[3–5] and supercapacitors.[6,7] Among various properties affected by nanoconfinement, the change in liquid diffusivity has attracted the vast majority of attention.[8–16] Typically, a large reduction in water diffusivity and the associated phase transition are observed when the thickness of a confined pure water film is reduced to a few molecular layers,[8–12,16,17] due to the confinement-induced low translational entropy of water molecules. Particularly, the formation of ice at room temperature, with an extremely low diffusion rate, was suggested for water sandwiched between the tip of a friction force microscope and a graphite substrate at appropriate tip–substrate separations.[17]

Resembling the case of pure water, aqueous electrolyte solutions in nanoconfined spaces also exhibit structures and dynamics different from those in the bulk. Consider, for example, the diffusion of ions and water molecules in nanoconfined salt solutions with respect to those in the bulk. As a baseline, the experimentally measured diffusion coefficients for alkali metal ions in dilute aqueous bulk solutions at 298 K are in the range of 1.0×10^{-5} cm^2 s^{-1} to 2.1×10^{-5} cm^2 s^{-1},[18] slightly lower than that of pure bulk water at 2.3×10^{-5} cm^2 s^{-1}.[19] The lower ion diffusivity is associated with the presence of a hydration shell around the ion, making its effective radius larger than that of the bare ion as well as the radius of an individual water molecule.[20] The consequence of the larger effective radius is a slower diffusion of the hydrated ion according to the Stokes–Einstein law.[21] In the case of nanoconfinement, the hydration shell may be partially shredded or flattened due to its interaction with confining solid surfaces, giving rise to a wide variety of anomalous ion diffusion activities. Examples are the observed enhancement or suppression in ion diffusion in confined salt solutions between two plates[22–25] and inside nanopores or nanochannels,[26,27] with respect to ion diffusion in bulk solutions. Additionally, ion diffusion in confined spaces depends also on the viscosity, concentration and temperature of the solutions, as well as the geometry and chemistry of the confining surfaces. However, despite dispersing over a wide range, all the reported diffusion coefficients for nanoconfined ions were relatively lower than that of water molecules in the same confined solution,[22–26] thus maintaining the trend in the bulk.[18,19] This unified picture is partially the result of all these confined salt solutions being in a liquid state. However, how confined ions behave when trapped in a solid-like crystal is poorly understood.

In the present study, we show by comprehensive molecular dynamics (MD) simulations that small alkali metal ions like

State Key Laboratory of Mechanics and Control of Mechanical Structures and Key Laboratory for Intelligent Nano Materials and Devices of MOE, Institute of Nano Science, Nanjing University of Aeronautics and Astronautics, Nanjing, 210016, China. E-mail: qiuhu@nuaa.edu.cn, wlguo@nuaa.edu.cn

†Electronic supplementary information (ESI) available: Snapshots of the confined solutions in liquid and solid-like states, additional simulation results of ion diffusion in a bulk ice crystal as well as in confined bilayer ice crystals obtained from simulations with the *NPT* ensemble, the TIP4P water model or a different set-up of wall parameters (PDF). Video showing the lateral hopping of a sodium ion along the lattice of a bilayer ice crystal (MPG). See DOI: 10.1039/C8NR01301B

Na^+ or Li^+ diffuse exceedingly faster than water molecules in a solid-like ice bilayer formed by laterally compressing a salt solution confined between two parallel walls. Our further analyses show that the faster ion diffusion can be attributed to the frequent lateral hopping of ions along the coordination sites formed between two water planes of the ice bilayer.

2. Methods

The simulation system used in the present study consists of aqueous solutions of alkali metal chlorides confined between two infinite parallel walls, as shown in the bottom inset in Fig. 1a. The wall–wall separation was chosen to be 0.9 nm, defined as the separation between the centers of mass of the atoms in the two walls. All wall atoms were placed in a monolayer with a triangular arrangement and a bond length fixed to 0.23 nm. The two walls were placed parallel to the (x, y) plane, equidistant from $z = 0$, and were fixed during all the simulations. Periodic boundary conditions were applied in the x and y directions to simulate the confinement by two infinite parallel walls, and a vacuum layer was used in the z direction to prevent direct interactions between water in adjacent periodic images in this direction. The length of the simulation cell in the x and y directions is 8.2 nm. Simulations were performed in an *NVT* ensemble, where the number of particles (N), volume (V) and temperature (T) of each system were kept constant. A series of systems containing various numbers of water molecules and ions were created to explore the properties of confined solutions at nominal densities ranging from 0.87 g cm^{-3} to 1.39 g cm^{-3}. The resulting lateral pressure in these *NVT* simulations was found to gradually increase to a few hundreds of MPa at high solution densities (ESI, section I†). The technique of varying the solution density to simulate the compression by lateral pressures has been widely used in many previous studies.[10,11,14,16,28] We also carried out a set of simulations in the *NPT* ensemble, with a constant lateral pressure being maintained, and observed a similar trend in diffusion enhancement at high lateral pressures (ESI, section I†). It is expected that, in future AFM experiments measuring the properties of a confined salt solution, a high density (or lateral pressure) could be achieved by filling the AFM chamber with a compressed high-pressure gas.

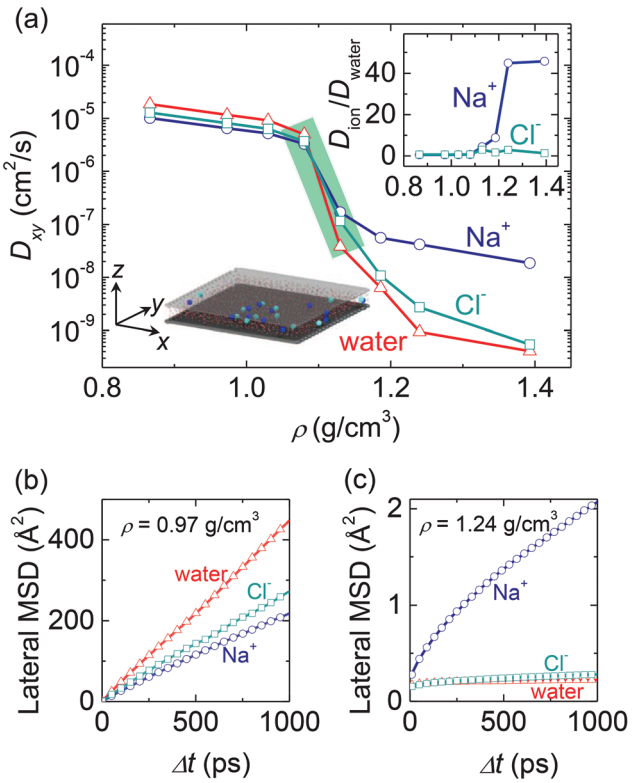

Fig. 1 Anomalous diffusion of ions in confined aqueous NaCl solutions. (a) Lateral diffusion coefficient D_{xy} as a function of the density ρ of NaCl solutions confined at a wall–wall separation of 0.9 nm. The top inset shows the ratio between diffusion coefficients of ions and water, D_{ion}/D_{water}, referred to as the diffusion enhancement factor of ions. The bottom inset shows the simulation system consisting of Na^+ (blue) and Cl^- (cyan) ions in an aqueous solution (red) confined between two parallel walls (grey). The upper wall was made transparent for clearer visualization. The coordinate origin was placed at the center of the system. (b) Lateral mean squared displacement (MSD) of water molecules, Na^+ and Cl^- ions at a low density ρ = 0.97 g cm^{-3} as a function of time separation Δt. (c) Same as (b) but at a high density ρ = 1.24 g cm^{-3}.

All MD simulations were carried out using Gromacs 5.1.4 software package,[29] and visualized and analyzed using VMD.[30] The TIP5P water model[31] was used to describe water, and a test simulation with the TIP4P water model[32] also yielded an enhancement in ion diffusion, though to a different extent (Table S2†). There is no charge assigned to wall atoms, and the van der Waals (vdW) interactions among water, ions and wall atoms was modeled by using a 6–12 Lennard-Jones (L-J) potential. The L-J parameters for ions were taken from those included in the OPLS-AA force field[33] and are provided in Table S1.† The L-J parameters for wall atoms were chosen to represent approximately the vdW interactions between the TIP5P water and a SiO_2 surface.[9,10] For a pair of atoms i and j, the L-J parameters between them were determined by combining the rules $\sigma_{ij} = (\sigma_{ii} + \sigma_{ij})/2$ and $\varepsilon_{ij} = \sqrt{(\varepsilon_{ii} \times \varepsilon_{jj})}$. For instance, the determined interaction parameters between water oxygen atoms and wall atoms are σ_{wall-O} = 0.316 nm and ε_{wall-O} = 0.831 kJ mol^{-1}. For the interaction between the hydrogen atoms of water and the wall atoms, the L-J parameters of σ_{wall-H} = 0.284 nm and ε_{wall-H} = 0.415 kJ mol^{-1} were adopted, as done in earlier studies.[9,10] We also performed an MD simulation with the minimum energy ε of wall atoms being modified to a value 10-fold smaller than its original value, and found about 20-fold faster Na^+ diffusion than water (see Table S2†). A time step of 2 fs was used. The Berendsen algorithm was employed to control the temperature at 300 K and the lateral pressure in *NPT* simulations.[34] vdW energies were calculated with a cutoff of 0.9 nm. A particle-mesh Ewald (PME) method was used to treat long-range electrostatics.[35] All other simulation parameters were identical to those implemented in our previous studies.[14,15] Each system was equilibrated for 30 ns, with the last 20 ns being used for

data analysis. At densities where a non-liquid phase was present, the equilibration time was extended to 300 ns to ensure adequate positional sampling of water and ions.

The lateral (in the (x–y) plane) diffusion coefficient D_{xy} was determined from the lateral MSD using the Einstein relationship

$$\mathrm{MSD}(\Delta t) = 4D_{xy}\Delta t. \quad (1)$$

The $\mathrm{MSD}(\Delta t)$ of each particle was averaged over snapshots from the whole MD trajectory with a time interval of Δt through the expression $\mathrm{MSD}(\Delta t) = \langle|\mathbf{r}(t + \Delta t) - \mathbf{r}(t)|^2\rangle$, where $\mathbf{r}$ represents the position of particles in the (x–y) plane and $\langle\ldots\rangle$ means the average over all particles of the same type.

3. Results and discussion

Fig. 1a shows the lateral diffusion coefficients, D_{xy}, for the three components (namely Na^+, Cl^- and water) in a 0.47 M NaCl solution as a function of the solution density ρ. At the lowest density (ρ = 0.87 g cm^{-3}), the confined solution is in a liquid state, as indicated by a high D_{xy} on the order of 10^{-5} cm^2 s^{-1} for all the three components. In this state, the D_{xy} for Na^+ (blue curve) or Cl^- (cyan curve) is lower than the D_{xy} for water (red curve), as generally expected for other confined[22–25] and bulk[36,37] solutions. As the ρ increases, the diffusion coefficients start to decrease smoothly from the order of 10^{-5} cm^2 s^{-1} to the order of 10^{-6} cm^2 s^{-1} until ρ = 1.08 g cm^{-3}. At this ρ range, the confined solution maintains its liquid state, as validated also by the fact that the mean square displacements (MSDs) of ions and water molecules all increase linearly with time at a moderate ρ of 0.97 g cm^{-3} (Fig. 1b). In addition, it is worth noting that ion diffusivities remain lower than water diffusivity in these liquid solutions. When the density approaches 1.13 g cm^{-3}, a sharp drop of more than an order in magnitude occurs simultaneously in all the three diffusion coefficient curves (highlighted by the tilted green rectangle in Fig. 1a). This sudden drop indicates that the confined liquid solution transforms into a solid-like crystal.

Upon the increase of ρ from 1.08 g cm^{-3} to 1.13 g cm^{-3} (highlighted by the tilted green rectangle), another particularly important fact is that the decrease in the Na^+ diffusion rate is less pronounced with respect to Cl^- or water. As a result, Na^+ diffusion becomes the fastest among the three components in the solution after the phase transition, in contrast to the trend in low-density confined solutions as well as in bulk solutions where Na^+ diffusion is the slowest.[18,19] On further increase of ρ to beyond 1.13 g cm^{-3}, the decrease in Na^+ mobility becomes more and more slow with respect to those for Cl^- and water, and therefore the Na^+ curve starts to deviate upward from the other two curves. Eventually, at a high solution density (namely, $\rho \geq$ 1.24 g cm^{-3}), Na^+ diffuses with a rate on the order of 10^{-8} cm^2 s^{-1}, much faster than those for water and Cl^- on the order of 10^{-9} cm^2 s^{-1} or 10^{-10} cm^2 s^{-1}. Note that the MSDs in the solid-like phase are not perfectly linear (Fig. 1c), indicating that it is not precisely accurate to extract diffusion coefficients from the slopes of these MSD plots. However, the obtained diffusion coefficients from this procedure could be adopted as a measure of the relative strength of the mobility.

Shown in the top inset of Fig. 1a is the diffusion enhancement factor of ions, D_{ion}/D_{water}, defined as the ratio between the diffusion coefficients for ions (D_{ion}) and water (D_{water}). In liquid solutions (*e.g.*, at $\rho \leq$ 1.08 g cm^{-3}), a Na^+ enhancement factor fluctuating around ~0.6 indicates its slightly slower diffusion than that of water, while in solid-like solutions (*e.g.*, $\rho \geq$ 1.24 g cm^{-3}), a factor of ~45 indicates an exceedingly faster diffusion for Na^+ with respect to water. In the case of Cl^-, a diffusion coefficient comparable to that of water was always present over the whole ρ range (cyan curve in Fig. 1a), as confirmed by the diffusion enhancement factor of Cl^- always fluctuating slightly around 1 (Fig. 1a, top inset).

It is known that a solid-like ice bilayer could be developed when water is confined at appropriate interplate spacings and subjected to an adequate increase in lateral pressures or solution densities.[10] Such an ice bilayer, observed also in the present confined solutions at high densities, is made of water molecules arranged with a rhombic in-plane symmetry forming a well-ordered hydrogen-bonding (HB) network, and therefore exhibits a low water mobility. When an ion is included in the lattice of the ice bilayer, the local HB network around the ion will be structurally and dynamically perturbed. As a consequence, the mobility of water molecules around the ion could be slightly enhanced, which, in turn, leads to a slight increase in the diffusivity of the ion itself. As an example, the diffusion coefficients for water in hydration shells of Na^+ and Cl^- ions trapped in the ice bilayer at ρ = 1.24 g cm^{-3} were determined to be 0.21×10^{-8} cm^2 s^{-1} and 0.14×10^{-8} cm^2 s^{-1}, respectively, slighter higher than that averaged over all water molecules in the solution (0.09×10^{-8} cm^2 s^{-1}).

Although Na^+ and Cl^- both exhibit faster diffusion than water in the bilayer ice, it is interesting to note that the diffusion coefficient for Na^+ is about an order of magnitude higher than that for Cl^- in the same confined solution (Fig. 1). The underlying mechanism could be understood by exploring the microscopic dynamics of these two ions in confined solutions. We first compare the transverse density distribution (namely, normal to the wall surface) of water oxygen atoms (Fig. 2a) and ions (Fig. 2b) in confined solutions at ρ = 0.97 g cm^{-3} (dashed curves) and ρ = 1.24 g cm^{-3} (solid curves). The bilayer nature of the confined solution could be confirmed by the observation of two evident peaks in oxygen density profiles (Fig. 2a) and two water planes in instantaneous MD snapshots (Fig. S3a and S3b in section II of the ESI†). Despite sharing similar density profiles (Fig. 2a), a bilayer liquid phase could be readily derived from the observed irregular arrangement of the positions of water oxygen atoms at low ρ (Fig. S3a†). In contrast, an ordered arrangement at high ρ, with an in-plane rhombic symmetry, reflects a solid-like bilayer crystalline phase (Fig. S3b†), in good agreement with a previous study.[10] As for the density distribution of ions (Fig. 2b), Na^+ and Cl^- display dramatically different trends from each other. Specifically, in the liquid solution at ρ = 0.97 g cm^{-3}, we found

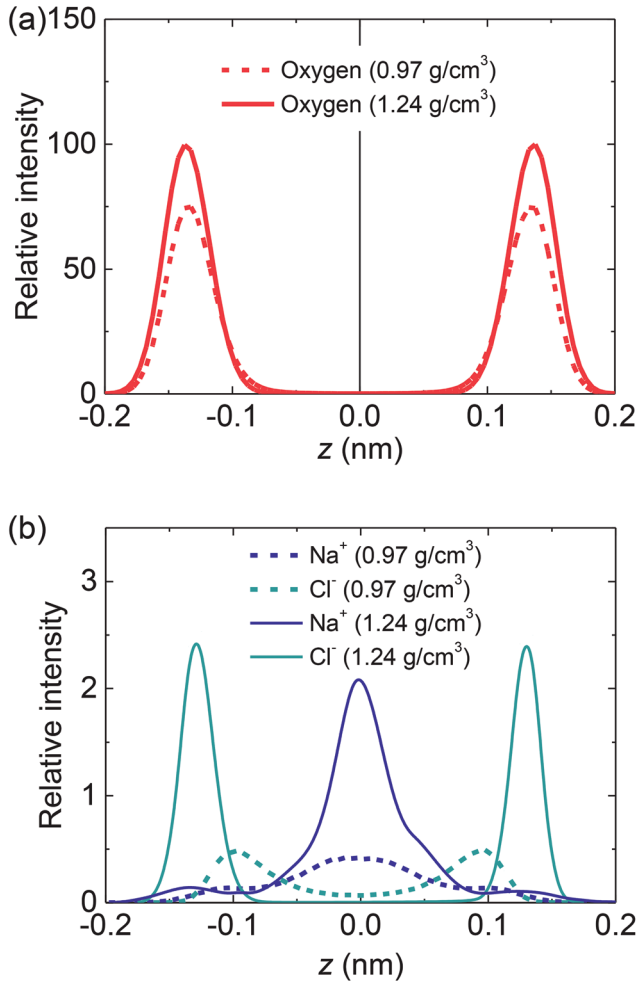

Fig. 2 Density distribution in confined salt solutions. (a, b) Transverse density profile of oxygen atoms of water (a) and ions (b) in low-density (dashed curves) and high-density (solid curves) NaCl solutions.

a single evident peak for Na^+ located in the middle plane of the system at $z = 0$ (blue dashed curve in Fig. 2b) but two peaks for Cl^- that deviate slightly from the middle plane (cyan dashed curve in Fig. 2b); in other words, Na^+ tends to reside in the space between two water planes forming the ice bilayer while Cl^- prefers to stay in close contact with the water planes. In the solid-like solution at $\rho = 1.24$ g cm^{-3} (blue solid curve in Fig. 2b), on the other hand, the Na^+ peak rises up with respect to that at $\rho = 0.97$ g cm^{-3}, and no evident positional shift is observed. Besides this main peak, we also note two small but clear secondary peaks/shoulders at the positions of the two oxygen planes. In contrast to the Na^+ distribution, the two peaks for the Cl^- density at $\rho = 1.24$ g cm^{-3} (cyan solid curve in Fig. 2b) were found to further move away from the middle plane, and eventually arrive at a position where the water density curve also shows peaks (red solid curve in Fig. 2a). This observation indicates that Cl^- prefers to embed into either of the water planes forming the ice bilayer.

To further characterize the dynamics of individual ions trapped in the bilayer ice, the time evolution of the z coordinate for each Na^+ and Cl^- in a typical 300 ns simulation is plotted in Fig. 3a and b, respectively. All the Na^+ curves can be divided into two categories with features distinct from each other (Fig. 3a). Specifically, a majority of Na^+ ions were found to wave slightly around the middle plane of the system at $z = 0$, with amplitudes less than 0.5 Å, while a few others exhibited large fluctuations with an amplitude of ~1.2 Å (see, for example, purple and dark blue curves in Fig. 3a). We note that a higher magnitude (*i.e.*, absolute value) of z than 1 Å corresponds to an "in-plane" configuration (highlighted in light brown), in which Na^+ steadily embeds into either of the two water planes forming the bilayer ice (see Fig. 3c, top panel). In parallel, a lower magnitude of z than 1 Å (highlighted in light green) represents an "off-plane" configuration, in which Na^+ ions reside in the space between the two water planes (see Fig. 3c, bottom panel). As for Cl^-, all ions in the solution adopted the in-plane configuration throughout the 300 ns

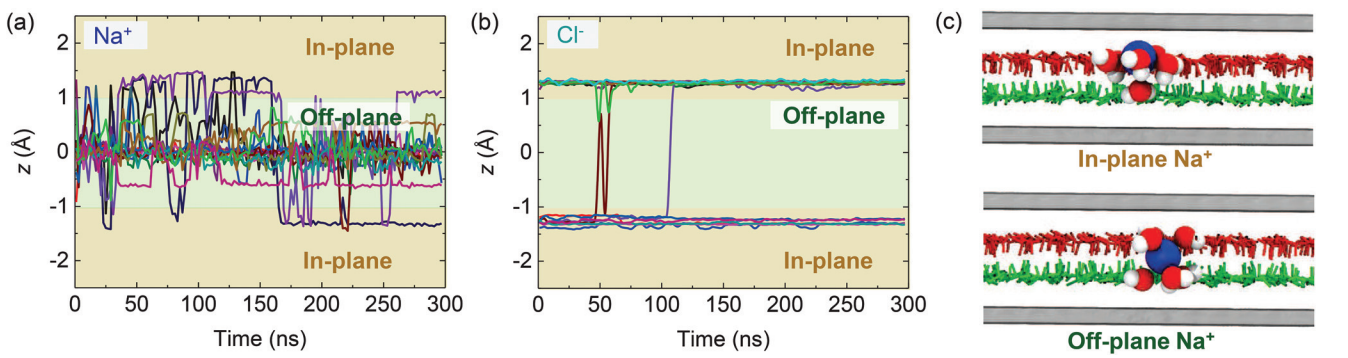

Fig. 3 Transverse displacement of Na^+ and Cl^- ions trapped in an ice bilayer. (a, b) The z coordinates of each Na^+ (a) and Cl^- (b) as a function of time in a 300 ns MD simulation. The two regions of ions residing in either of the two water planes (*i.e.*, in-plane) are highlighted in light brown rectangles, while the in-between light green rectangles represent regions where ions deviate from the water planes (*i.e.*, off-plane). (c) Side-view snapshots showing a Na^+ ion at the in-plane configuration (top) and another Na^+ ion at the off-plane configuration (bottom). Na^+ ions and oxygen atoms of the water molecules surrounding the ions are shown in sphere representation, with Na^+ in blue and oxygen atoms in red.

Table 1 Probability distribution of ion configurations and their corresponding lateral diffusion coefficients

	Configuration	Percentage (%)	D_{xy} (10^{-8} cm^2 s^{-1})
Na^+	In-plane	11.4	0.52
	Off-plane	88.6	4.85
Cl^-	In-plane	99.2	0.26
	Off-plane	0.8	—

simulation, with rare exceptions observed when Cl^- ions hopped from one water plane to the other (Fig. 3b).

The probability of ions adopting the two observed configurations and the corresponding diffusion coefficients are summarized in Table 1. It is found that Na^+ takes the off-plane configuration with a high probability at 88.6%, and the determined diffusion coefficient for this configuration is approximately an order of magnitude higher than that for the rarely observed in-plane configuration (at a probability of 11.4%). By comparison, Cl^- ions prefer to embed into the water plane adopting the in-plane configuration (at a probability of 99.2%). The positional distribution of ions is in line with the trend reflected in the density profiles (Fig. 2b). Furthermore, it is interesting to note that the diffusion coefficient for the in-plane Cl^- is comparable to that for the in-plane Na^+, but about an order of magnitude lower than that of the off-plane Na^+ (Table 1). This result further confirms that the faster Na^+ diffusion originates from its high preference to stay far away from the water plane, a configuration maintaining high mobility. The different dynamics demonstrated for Na^+ and Cl^- clearly indicate distinct interactions of these two ions with surrounding water molecules or wall surfaces. In particular, the water molecules in the bilayer ice have a preferential orientation and therefore exhibit a non-zero quadruple moment, giving rise to different interactions with cations (such as Na^+) and anions (such as Cl^-). This effect was shown to induce a few interesting observations such as access of anions next to hydrophobic plates.[38] In addition, we expect that the present findings could be extended to a trilayer system, because trilayer ice was found to appear for certain plate separations at high lateral pressures,[39] although trilayer liquid water was observed in these systems at ambient pressures.[40]

An interesting issue regarding the aforesaid anomalous ion diffusion is to know how Na^+ achieves the predicted high mobility for the off-plane configuration. Fig. 4a shows the path lines of two typical Na^+ ions along the (x, y) direction within a 20 ns duration: an in-plane Na^+ (brown) and an off-plane Na^+ (green). It is found that the in-plane Na^+ fluctuates slightly around its original site with very rare hopping events. This is partially because the lateral movement of Na^+ in this configuration would involve significant motion of surrounding water such as the exchange of neighboring water molecules with this ion, a process that needs to overcome large energy barriers. In stark contrast, the off-plane Na^+ exhibits a number of hopping events from one coordinate site to the next, leading to a more widespread distribution of Na^+ positions in the (x, y) plane

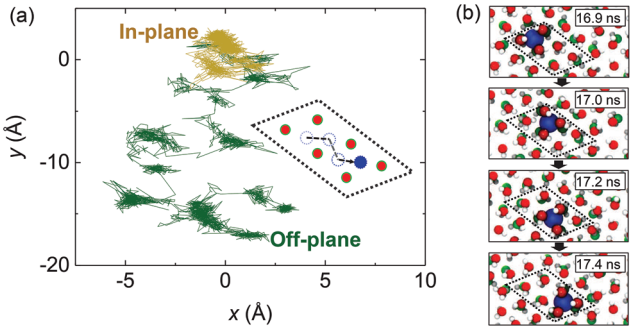

Fig. 4 Mechanism of fast Na^+ diffusion. (a) The in-plane path lines (in the (x, y) plane) of an in-plane Na^+ (brown) and an off-plane Na^+ (green) in a 20 ns trajectory when both ions were trapped in the lattice of an ice bilayer. The Na^+ position (x, y) at the beginning of the trajectory was set as (0, 0). (b) Top-view snapshots showing three sequential hopping events of an off-plane Na^+ occurring in a 0.5 ns duration. A schematic of the hopping trace of this ion is provided in the inset of panel a.

than that for the in-plane Na^+ (Fig. 4a). A few such typical events are highlighted in the MD snapshots shown in Fig. 4b (see also the Supplemental Video in the ESI†) and in a schematic diagram shown in the inset of Fig. 4a. Initially, a Na^+ ion (blue) in its coordination site was surrounded by six adjacent water molecules forming a "triangular prism" (topmost panel), with three water molecules contributed by the upper water plane (red) and the other three by the lower water plane (green). This Na^+ ion can hop progressively between its original "triangular prism" and contiguous "prisms" formed by neighboring water molecules, with each hopping event occurring typically on the time scale of a few hundreds of picoseconds. It is noteworthy that such Na^+ hopping does not involve any significant movement or rearrangement of neighboring water molecules, thus overcoming lower energy barriers compared to the Na^+ movement in the in-plane configuration. As a result, the frequent hopping of Na^+ in the off-plane configuration leads to the fast Na^+ diffusion predicted above.

To examine the proposed mechanism for the anomalous ion diffusion, we compared the results from a series of MD simulations on confined solutions of different alkali metal chlorides including LiCl, NaCl, KCl, RbCl and CsCl. At a low density (ρ = 0.97 g cm^{-3}), a diffusion enhancement factor (D_{ion}/D_{water}) less than 1 for all these cations suggests a slower diffusion with respect to water (see the inset in Fig. 5a). At a high density (ρ = 1.24 g cm^{-3}), the smallest alkali metal ion Li^+ was found to also diffuse notably faster than water, similar to the case of Na^+, with a diffusion enhancement factor at 30.9 (Fig. 5a). By comparison, the diffusion enhancement for larger alkali metal ions including K^+, Rb^+ and Cs^+ is much weaker than that for smaller ions, indicated by low diffusion enhancement factors not exceeding 10. In particular, no evident enhancement in ionic diffusion was seen for the two largest ions Rb^+ and Cs^+, as indicated by a low enhancement factor around 2. In Fig. 5b, we plot the fraction of these cations adopting the in-plane configuration in solutions

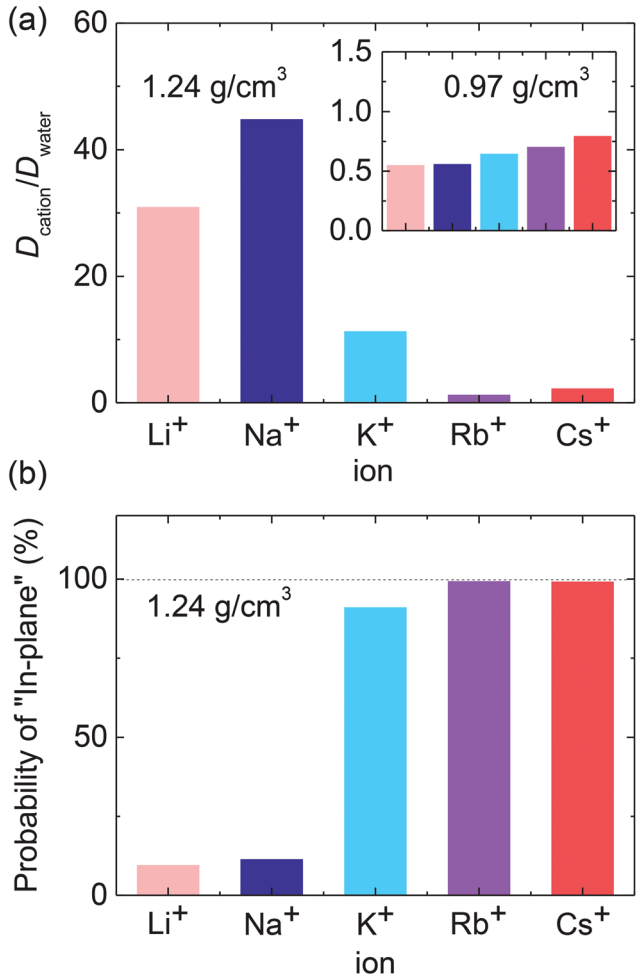

Fig. 5 Diffusion of different alkali metal ions trapped in an ice bilayer. (a, b) The diffusion enhancement factor of ions, D_{ion}/D_{water}, for cations in 0.47 M aqueous solutions of LiCl, NaCl, KCl, RbCl and CsCl at ρ = 1.24 g cm^{-3}. The inset shows the same group of data but at ρ = 0.97 g cm^{-3}. (b) Probability of different alkali metal ions adopting the in-plane configuration in confined solutions at ρ = 1.24 g cm^{-3}.

at ρ = 1.24 g cm^{-3}. It is clear that an inverse relationship is present between an ion's diffusion enhancement (Fig. 5a) and its affinity to the in-plane configuration (Fig. 5b). For instance, the two smallest ions, Li^+ and Na^+, both have a low probability of around 10% to embed into either of the water planes; in other words, these two ions prefer to adopt the more mobile off-plane configuration (at a probability of about 90%) because they can fit well with the "triangular prism" formed between the two water planes (see Fig. 4b), leading to their fastest diffusion rates among all the alkali metal ions (Fig. 5a). In contrast, larger cations K^+, Rb^+ and Cs^+ cannot fit well within the "triangular prism" and therefore have a probability of higher than 90% to embed into either of the water planes, namely adopting the less-mobile in-plane configuration. As a result, a quite low diffusion enhancement was observed for these three large ions (Fig. 5a). Note that K^+ has a relatively low probability of ~91% for the in-plane configuration than those for Rb^+ and Cs^+ at ~99%, resulting in a relatively higher diffusion enhancement factor for K^+ over Rb^+ and Cs^+.

It is generally accepted that an extremely low solubility is present for salts in bulk ice crystals, that is, most salt ions are rejected from aqueous salt solutions upon freezing.[41,42] On the other hand, a small amount of salt ions can be accommodated in the lattice of the ice, giving rise to the so-called ice doping.[43,44] Earlier work suggested that an increase in the salt concentration[45] or a decrease in temperature[44] could increase the amount of trapped ions in ice crystals. In the present study, a sudden increase in the density (equivalent to a sudden increase in the lateral pressure) was used to induce the transition of a bilayer liquid to a bilayer solid. Note that this transition occurs rapidly on the time scale of a few nanoseconds, mostly due to the presence of an extreme confinement. As a result, ions were not seen to be rejected from the ice crystal, but instead, were eventually trapped at different sites inside the HB network formed by water molecules (see Fig. 4b). Such trapping of ions inside a solid-like crystal was also found in a very recent simulation of a bulk NaCl solution.[44] In that work, no evident diffusion of ions was observed, even though the simulation lasted up to a few microseconds. Similarly, we carried out a test simulation of ions trapped in the lattice of a bulk ice crystal and found no significant enhancement in ion diffusion (ESI, section III†).

4. Conclusions

In summary, we revealed an anomalous cation diffusion with respect to the diffusion of water molecules when ions are trapped in the lattice of a confined ice bilayer by comprehensive MD simulations. In particular, the diffusion enhancement of small alkali metal ions such as Li^+ and Na^+ is the most significant because they have a high preference to reside in the interlayer space between the two water planes forming the ice bilayer, a configuration found to be highly mobile due to the frequent lateral hopping of ions inside the ice bilayer. In contrast, the diffusion enhancement of larger cations K^+, Rb^+ and Cs^+ as well as anion Cl^- is not as significant as that for Li^+ and Na^+, because the former prefer to embed into either of the two water planes, a configuration that suppresses diffusion. The present findings should extend our understanding of the diffusive dynamics of solutes in solutions under confinement.

Conflicts of interest

There are no conflicts to declare.

Acknowledgements

This work was supported by the National Natural Science Foundation of China (11772152, 11402113, 51535005, and 51472117), the Jiangsu Province NSF (BK20140807), the Research Fund of State Key Laboratory of Mechanics and Control of

Mechanical Structures (MCMS-0417G03), the Fundamental Research Funds for the Central Universities (NJ20160103 and NP2017101), Funding of Jiangsu Innovation Program for Graduate Education (KYLX_0225), and a project funded by the Priority Academic Program Development of Jiangsu Higher Education Institutions. The authors acknowledge helpful discussions with Drs Zhuhua Zhang and Jianxin Zhou.

References

1 S. P. Surwade, S. N. Smirnov, I. V. Vlassiouk, R. R. Unocic, G. M. Veith, S. Dai and S. M. Mahurin, *Nat. Nanotechnol.*, 2015, **10**, 459–464.
2 M. Xue, H. Qiu and W. Guo, *Nanotechnology*, 2013, **24**, 505720.
3 S. Garaj, W. Hubbard, A. Reina, J. Kong, D. Branton and J. A. Golovchenko, *Nature*, 2010, **467**, 190–193.
4 M. Wanunu, *Phys. Life Rev.*, 2012, **9**, 125–158.
5 H. Qiu, A. Girdhar, K. Schulten and J.-P. Leburton, *ACS Nano*, 2016, **10**, 4482–4488.
6 C. Merlet, C. Péan, B. Rotenberg, P. A. Madden, B. Daffos, P.-L. Taberna, P. Simon and M. Salanne, *Nat. Commun.*, 2013, **4**, 2701.
7 X. Fan, C. Yu, J. Yang, Z. Ling, C. Hu, M. Zhang and J. Qiu, *Adv. Energy Mater.*, 2015, **5**, 1401761.
8 J. Gao, W. D. Luedtke and U. Landman, *Phys. Rev. Lett.*, 1997, **79**, 705–708.
9 R. Zangi and A. E. Mark, *Phys. Rev. Lett.*, 2003, **91**, 025502.
10 R. Zangi and A. E. Mark, *J. Chem. Phys.*, 2003, **119**, 1694–1700.
11 S. Han, M. Choi, P. Kumar and H. E. Stanley, *Nat. Phys.*, 2010, **6**, 685–689.
12 S. H. Khan, G. Matei, S. Patil and P. M. Hoffmann, *Phys. Rev. Lett.*, 2010, **105**, 106101.
13 J. Bai and X. C. Zeng, *Proc. Natl. Acad. Sci. U. S. A.*, 2012, **109**, 21240–21245.
14 H. Qiu, X. C. Zeng and W. Guo, *ACS Nano*, 2015, **9**, 9877–9884.
15 H. Qiu and W. Guo, *Phys. Rev. Lett.*, 2013, **110**, 195701.
16 N. Giovambattista, P. J. Rossky and P. G. Debenedetti, *Phys. Rev. Lett.*, 2009, **102**, 050603.
17 K. B. Jinesh and J. W. M. Frenken, *Phys. Rev. Lett.*, 2008, **101**, 036101.
18 W. M. Haynes, D. R. Lide and T. J. Bruno, *CRC handbook of chemistry and physics*, Taylor & Francis Group, 97th edn, 2016.
19 M. Holz, S. R. Heil and A. Sacco, *Phys. Chem. Chem. Phys.*, 2000, **2**, 4740–4742.
20 S. Glasstone, *An introduction to Electrochemistry*, D. Van Nostrand Company, lnc., New York, 1962.
21 R. Mills and V. M. Lobo, *Self-diffusion in electrolyte solutions*, Elsevier, Amsterdam, 1989.
22 J. Kong, Z. Bo, H. Yang, J. Yang, X. Shuai, J. Yan and K. Cen, *Phys. Chem. Chem. Phys.*, 2017, **19**, 7678–7688.
23 T. A. Ho, D. Argyris, D. R. Cole and A. Striolo, *Langmuir*, 2012, **28**, 1256–1266.
24 M. Holmboe and I. C. Bourg, *J. Phys. Chem. C*, 2014, **118**, 1001–1013.
25 S. Kerisit and C. Liu, *Environ. Sci. Technol.*, 2009, **43**, 777–782.
26 R. M. Lynden-Bell and J. C. Rasaiah, *J. Chem. Phys.*, 1996, **105**, 9266–9280.
27 X. Gao, T. Zhao and Z. Li, *J. Appl. Phys.*, 2014, **116**, 054311.
28 P. Kumar, S. V. Buldyrev, F. W. Starr, N. Giovambattista and H. E. Stanley, *Phys. Rev. E: Stat., Nonlinear, Soft Matter Phys.*, 2005, **72**, 051503.
29 M. J. Abraham, T. Murtola, R. Schulz, S. Páll, J. C. Smith, B. Hess and E. Lindahl, *SoftwareX*, 2015, **1–2**, 19–25.
30 W. Humphrey, A. Dalke and K. Schulten, *J. Mol. Graphics*, 1996, **14**, 33–38.
31 M. Mahoney and W. Jorgensen, *J. Chem. Phys.*, 2000, **112**, 8910.
32 W. L. Jorgensen, J. Chandrasekhar, J. D. Madura, R. W. Impey and M. L. Klein, *J. Chem. Phys.*, 1983, **79**, 926–935.
33 W. L. Jorgensen, D. S. Maxwell and J. Tirado-Rives, *J. Am. Chem. Soc.*, 1996, **118**, 11225–11236.
34 H. J. C. Berendsen, J. P. M. Postma, W. F. van Gunsteren, A. DiNola and J. R. Haak, *J. Chem. Phys.*, 1984, **81**, 3684–3690.
35 U. Essmann, L. Perera, M. L. Berkowitz, T. Darden, H. Lee and L. G. Pedersen, *J. Chem. Phys.*, 1995, **103**, 8577–8593.
36 S. Chowdhuri and A. Chandra, *J. Chem. Phys.*, 2001, **115**, 3732–3741.
37 A. Ghaffari and A. Rahbar-Kelishami, *J. Mol. Liq.*, 2013, **187**, 238–245.
38 R. Zangi, M. Hagen and B. J. Berne, *J. Am. Chem. Soc.*, 2007, **129**, 4678–4686.
39 F. Zhu and B. Chen, *J. Chem. Inf. Model.*, 2015, **55**, 1361–1368.
40 R. Zangi, *J. Phys.: Condens. Matter*, 2004, **16**, S5371–S5388.
41 G. W. Gross, P. M. Wong and K. Humes, *J. Chem. Phys.*, 1977, **67**, 5264–5274.
42 M. A. Carignano, P. B. Shepson and I. Szleifer, *Chem. Phys. Lett.*, 2007, **436**, 99–103.
43 J. R. Addison, *J. Appl. Phys.*, 1969, **40**, 3105–3114.
44 M. M. Conde, M. Rovere and P. Gallo, *Phys. Chem. Chem. Phys.*, 2017, **19**, 9566–9574.
45 L. Vrbka and P. Jungwirth, *Phys. Rev. Lett.*, 2005, **95**, 148501.

